Heavy Ion Results from ATLAS

Jiangyong Jia on behalf of the ATLAS Collaboration[1]

Chemistry Department, Stony Brook University, NY 11794, USA; Physics Department, Brookhaven National Laboratory, NY 11796, USA

Abstract

These proceedings provide an overview of the new results obtained with the ATLAS detector at the LHC, which were presented in the Quark Matter 2017 conference. These results were covered by twelve parallel talks, one flash talk and eleven posters. These proceedings group these results into five areas: initial state, jet quenching, quarkonium production, longitudinal flow dynamics, and collectivity in small systems.

Keywords: ATLAS, heavy-ion collisions, quark-gluon plasma, jet quenching, flow decorrelation, multi-particle cumulants

1. Introduction

In order to reliably extract the properties of the Quark Gluon Plasma (QGP) created in heavy ion collisions at the LHC, one needs to first achieve a detailed understanding of the space-time evolution of the system. This requires improving the precision of the measurements on existing observables, exploring new observables, as well as studying the dependence on the type of collision systems or the collision energies. In this conference, ATLAS showed many new results obtained from high statistics pp data at 2.76, 5.02 and 13 TeV, p+Pb data at 5.02 and 8.16 TeV, as well as Pb+Pb data at 2.76 and 5.02 TeV, collected in the Run 1 (2010–2013) and Run 2 (2015–2016) periods. These results range from constraining the initial state of the heavy ion collisions, to understanding the interaction of the hard probes with the QGP and the longitudinal expansion of the QGP, and to the clarification of the origin of collective behavior in small collision systems.

2. Initial state

Because of the strong electromagnetic field associated with the highly boosted nuclei at the LHC, Ultra Peripheral heavy-ion Collisions (UPC) can be used to study the scattering of the quasi-real photons emitted coherently from nuclei as they pass by each other. In Pb+Pb collisions, such photon-photon scattering processes are enhanced by a factor of $Z^4 \sim 4.5 \times 10^7$ compared to pp collisions. Two interesting processes, $\gamma\gamma \to \mu^+\mu^-$ and $\gamma\gamma \to \gamma\gamma$, have been measured by ATLAS [1]. These processes can be cleanly identified event by event, as the signal is usually associated with very simple final-state topology with very little additonal event activity. The differential cross-section for $\gamma\gamma \to \mu^+\mu^-$, proportional to α_{em}^2, is found to be well described by a leading order QED calculation provided by the STARlight model. The $\gamma\gamma \to \gamma\gamma$

process has significantly smaller cross section at lowest order, i.e $\propto \alpha_{em}^4$, due to the requirement of one-loop box diagrams involving fermions. Nevertheless, 13 events have been identified passing the fiducial kinematic cuts. The significance of the observation is 4.4σ, which agrees well with the 3.8σ expected from the QED calculation. Both measurements provide an important experimental constraint on photon fluxes in ultra-peripheral Pb+Pb collisions.

The UPC also provides a unique opportunity to study the parton distribution function in the colliding nuclei (nPDF) via the measurement of photo-nuclear dijet production [2], where one quasi-real photon is emitted coherently from one nucleus and scatters inelastically with the second nucleus and produces dijets in the final state: γ+Pb→dijets+X. The nucleus emitting the photon remains intact, while the other nucleus dissociates and produces fragments in the forward direction. Such events can be cleanly selected by requiring spectator neutrons detected only in one of the zero-degree calorimeters situated in the beam fragmentation region. Due to the relatively low p_T of the photon, this process is sensitive to the nPDF at low x in the Pb and moderate momentum transfer Q^2. Figure 1 shows the differential cross-section as a function of x for different H_T. The H_T is the scalar-sum of the p_T of the jets, therefore H_T^2 is a proxy for Q^2. The results from Fig. 1 span a x and Q^2 region not covered in previous measurements.

A more traditional way of constraining the nPDF is through the measurement of electro-weak bosons such as Z and W. ATLAS studied Z boson production in p+Pb and Pb+Pb collisions via the nuclear modification factors, $R_{p\mathrm{Pb}}$ and R_{AA}, respectively [3]. The η dependence of $R_{p\mathrm{Pb}}$ shows slight forward-backward asymmetry consistent with nuclear isospin effects. The R_{AA} in Pb+Pb collisions shows little modification as a function of either η or centrality. Thanks to the large integrated luminosity, the uncertainty of R_{AA} is no longer dominated by the Z yield as in the past, instead it is dominated by the uncertainty associated with the Glauber model. Given the lack of nuclear effects, the Z boson production with sufficient statistical precision may be used as an alternative baseline for studying the nuclear modification factors for other hard processes.
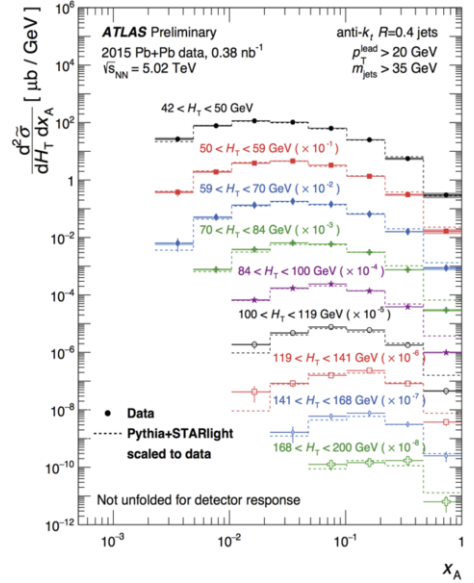

Figure 1. Differential cross-section $d\sigma/dH_T dx$ as a function of x for different bins of H_T. The dashed lines represent the cross-section from Pythia+STARlight scaled to have the same integral as the data within the fiducial region of the measurement.
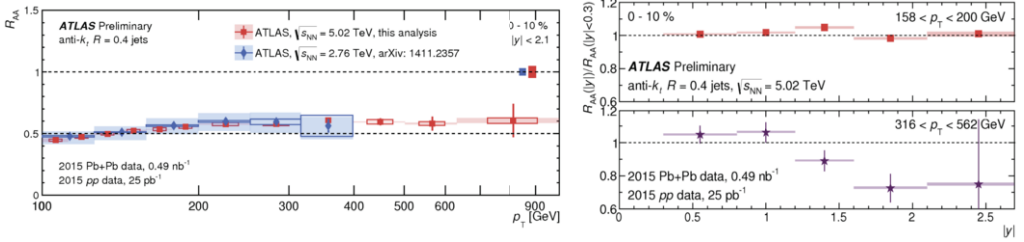
3. Jet quenching

Using the high statistics Pb+Pb data and pp reference data collected in Run 2, ATLAS made the first measurement of inclusive jet production at 5.02 TeV [4]. This result provides a detailed study of R_{AA} as a function of p_T, centrality and rapidity y. The R_{AA} in central collisions, as shown in Fig. 2 (left), reveals a clear increase with p_T and flattening behavior above 200–300 GeV. The behavior is consistent with the results at 2.76 TeV, but the systematic uncertainties are much reduced thanks to the cancellation of the uncertainty between pp and Pb+Pb. This cancellation is possible because the pp reference data are taken just prior to the heavy-ion run, and therefore have the same detector condition. The large statistics also allow the study of the evolution of R_{AA} as a function of rapidity, which is quantified via a double ratio: $R_{\mathrm{AA}}(|y|)/R_{\mathrm{AA}}(|y| < 0.3)$. Any deviation of this double ratio from one indicates a y dependence of R_{AA}. This ratio is observed in Fig. 2 (right) to be flat with y at low p_T, but for the first time, it is observed to decrease with y at high p_T. This behavior reflects an interplay between y-dependent composition and the spectral

Figure 2. Left: The R_{AA} as a function of p_T for jets with $|y| < 2.1$ in 0-10% central Pb+Pb collisions at 2.76 and 5.02 TeV. Right: The ratio of the R_{AA} as a function of $|y|$ to the R_{AA} at $|y| < 0.3$ for jets with centrality of 0-10% in a low p_T (red squares) and a high p_T (purple stars) region.

shape for quarks and gluons. The larger quark content at large y favors less suppression, which is probably over-compensated by the much steeper parton spectral shape which favors more suppression.

Further information about jet quenching can be obtained from measurement of jet substructure, e.g. the jet Fragmentation Function (FF). ATLAS measured the jet FF $D(z)$ in p+Pb collisions as a function of
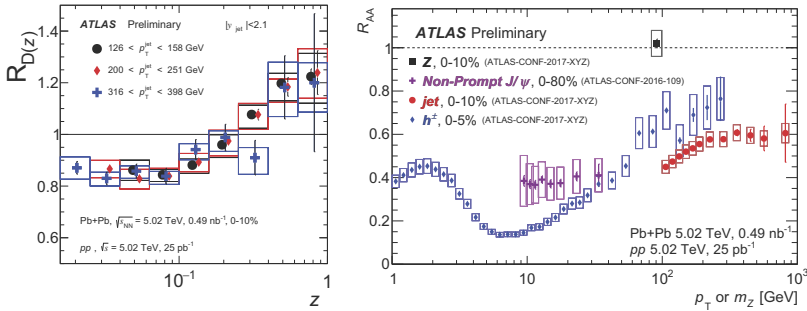

Figure 3. Left: Modificaition of fragmentation function for three jet p_T in 0-10% central Pb+Pb collisions at 5.02 TeV. Right: Compilation of results for R_{AA} vs. p_T in different channels from the Run 2 data.

$z = p_T/p_{Tjet}$, momentum fraction of charged particle [5, 6]. The FF is found to be not modified with respect to pp collisions. However in central Pb+Pb collisions as shown by Fig. 3(left), the FF is found to be strongly modified. The FF shows a suppression at intermediate $z \sim 0.1$ and 10–20% enhancement at higher z. The suppression is found to be independent of the jet energy, and for the same jet energy the results are also found to be similar between $\sqrt{s_{NN}} = 2.76$ and 5.02 TeV. From the same pp and Pb+Pb datasets, ATLAS also measured the suppression of inclusive charged hadrons from 1– 300 GeV (Fig. 3(right)) [4]. The R_{AA} at higher p_T is below one but is slightly above the R_{AA} for inclusive jets. This is expected, as most high p_T hadrons come from the high z region where the FF is enhanced.
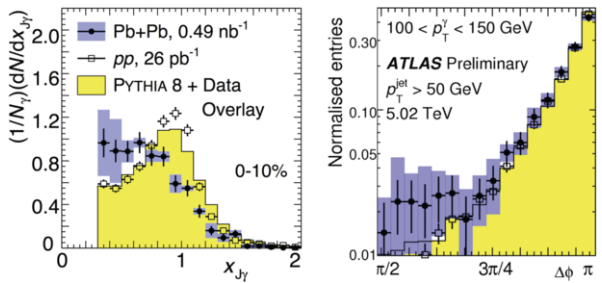

Figure 4. Distributions of the jet-to-photon transverse momentum ratio $x_{J\gamma}$ (left panel) and relative azimuthal angle (right panel) in Pb+Pb data (filled circles), pp (open squares), and Pythia 8 simulation (yellow histogram).

One golden observable for the jet quenching effect is the modification of the jets tagged by high p_T direct photons, or γ-jet correlations. The relevant observables are the momentum imbalance between the γ and jet, $x_{J\gamma} = p_{Tjet}/p_{T\gamma}$, as well as the azimuthal angle correlation between the γ and the jet. The results for pp

and central Pb+Pb collisions are summarized in Fig. 4 [7]. The $x_{J\gamma}$ distribution is observed to be strongly shifted to lower value with respect to the distribution for pp collisions, which implies a strong energy loss for the jet associated with the γ. However the azimuthal angle distribution implies that the jet direction is not modified with respect to pp.

4. Quarkonium production

ATLAS has performed a detailed study of the nuclear modification factor for charmonium states J/Ψ and Ψ(2s) in pp, p+Pb and Pb+Pb collisions [8] and bottomonium states Υ in pp and p+Pb collisions [9]. The charmonium states are measured in the range of $p_T > 9$ GeV, and they are separated into the prompt and non-prompt components based on the pseudo proper time distribution. The non-prompt component is dominated by the feed-down contribution from bottom hadrons, while the prompt component arises from thermal production as well as jet fragmentations. These two components are observed to be suppressed slightly differently as a function of p_T: the prompt J/Ψ shows less suppression at higher p_T, while the suppression for non-prompt J/Ψ is found to be independent of p_T. Due to limited statistics, the suppression

of Ψ(2s) is measured relative to that for J/Ψ via a double ratio $R_{AA}^{\Psi(2s)}/R_{AA}^{J/\Psi}$, which has the advantage of cancelling a large part of the systematic uncertainties. The results are shown in Fig. 5. For the prompt component, the Ψ(2s) is found to be more suppressed than the J/Ψ. For the non-prompt component, the Ψ(2s) and J/Ψ show similar suppression, which is expected as both are created outside the QGP from decay of bottom hadrons.
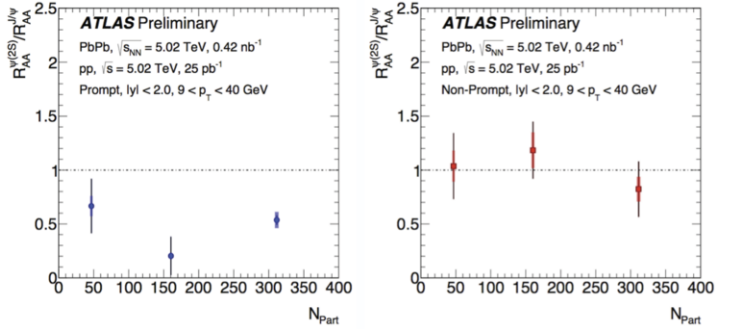

Figure 5. Ratio of R_{AA} for J/Ψ and R_{AA} for Ψ(2s), as a function of centrality for prompt meson production (left) and non-prompt meson production (right) in Pb+Pb collisions at 5.02 TeV.

5. Longitudinal flow fluctuations in Pb+Pb collisions

In the past, most studies of collective flow only considered the transverse dynamics, and expansion of the QGP in the longitudinal direction is often assumed to be boost invariant. However, since the shape of the produced fireball depends on the distributions of participating nucleons in the forward and backward-going nuclei, both the amplitude and phase of the harmonic flow should vary as a function of rapidity in each event, and the produced system is inherently not boost invariant. Recent model studies revealed strong fluctuations of the flow magnitude and phase between two well separated pseudorapidities, i.e. $v_n(\eta_1) \neq v_n(\eta_2)$ (forward-backward asymmetry) and $\Phi_n(\eta_1) \neq \Phi_n(\eta_2)$ (event-plane twist) [10, 11].

ATLAS measured these flow decorrelation effects in 2.76 TeV and 5.02 TeV Pb+Pb collisions using many observables proposed in Ref. [12]. One of those is a generalization of correlator first used by the CMS Collaboration [13]

$$r_{n|n;k}(\eta) = \frac{\left\langle [v_n(-\eta)v_n(\eta_{\text{ref}})]^k \cos kn(\Phi_n(-\eta) - \Phi_n(\eta_{\text{ref}})) \right\rangle}{\left\langle [v_n(\eta)v_n(\eta_{\text{ref}})]^k \cos kn(\Phi_n(\eta) - \Phi_n(\eta_{\text{ref}})) \right\rangle}, \tag{1}$$

which quantifies the decorrelation between η and $-\eta$ using a common reference rapidity η_{ref}. Figure 6 shows the results of $r_{n|n;1}$ for n=2,3 and 4. A strong decorrelation that depends linearly on η is observed.
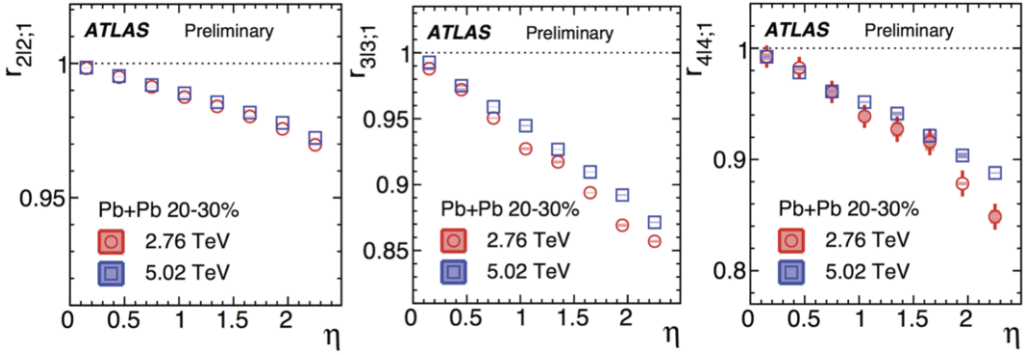
Figure 6. The $r_{n|n;1}(\eta)$ in 20–30% centrality Pb+Pb collisions for $n = 2$,3 and 4 from left to right, compared between the two collision energies.

The decorrelation is found to be stronger in 2.76 TeV than 5.02 TeV. The slope of this linear dependence is found to be 10% larger for v_2 but is about 16% larger for v_3 and v_4, and they are found to be independent of the event centrality. These results should provide strong constraints on the energy dependence of initial conditions for the hydrodynamic models, which have been used to make predictions for the decorrelation effects at RHIC energies. The fact that energy dependence is stronger for v_3 than that for v_2 may suggest some non-trivial stopping mechanisms for the colliding nuclei.

There are a lot more results from ATLAS on longitudinal flow decorrelations, which can not be covered by this overview talk. These results can be divided into three areas: Firstly, the results shown in Fig. 6 are extended to the second moment $k = 2$ and the third moment $k = 3$, which are sensitive to the EbyE fluctuation of the flow decorrelations. The slope for the kth-moment is found to scale with k for $n > 2$, but it scales faster than k for $n = 2$. Secondly, a correlation between four subevents in different η intervals is measured to separate the contributions from fluctuation of the v_n amplitude and fluctuation of Φ_n. Both contributions are found to be comparable to each other. Thirdly, correlations between harmonics of different order, e.g. between v_2 and v_4 in different η intervals, are also measured to investigate how the mode-mixing effects evolve with rapidity. The correlations between v_4 and v_2^2 suggest that the longitudinal fluctuations of v_4 are driven by a non-linear contribution from v_2, i.e. $v_4 \propto v_2^2$. Similarly, the correlations between v_5 and $v_2 v_3$ suggest that the longitudinal fluctuations of v_5 are driven by a non-linear contribution from $v_2 v_3$, i.e. $v_5 \propto v_2 v_3$. These measurements provide important insights on the EbyE fluctuations, as a function of η, of the initial conditions as well as the non-linear mode-mixing effects. Details of these results can be found in the two proceedings [14, 15].

6. Collectivity in small collisions system

One active area of current research concerns the nature of the long-range ridge observed in two-particle correlation (2PC) in small collision systems, namely pp, pA, and low multiplicity A+A collisions. The ridge is a $\Delta\phi$ correlation between particle pairs that extends to very large $\Delta\eta$, and properties of the ridge are often quantified via a Fourier expansion $dN/d\Delta\phi \sim 1 + 2 \sum_n v_n^2 \cos n\Delta\phi$. There are extensive ongoing experimental efforts to systematically map out the differential information of v_n as a function of p_T, particle species, $\sqrt{s}$ and collision systems. In ATLAS, the v_n harmonics are obtained from a 2PC analysis [16, 17], where the non-flow effects for events in a multiplicity range, mostly from inter-jet correlations from di-jets, are estimated using low-multiplicity events and then subtracted. The subtraction was done by either including or not including the pedestal in the low multiplicity events (labelled as "template fit" and "peripheral subtraction" respectively), where the pedestal is determined by a zero-yield at minimum (ZYAM) procedure [18]. Not including the pedestal in low-multiplicity events in the subtraction was shown [17] to significantly reduce the measured v_2 value, since it explicitly assumes no long-range v_2 in the peripheral bin and therefore forces the v_2 to be zero at the lowest multiplicity. Therefore, ATLAS chooses the template fit method as the default 2PC method for v_n measurement.

Figure 7 (left) shows a compilation of v_2 (the dominating harmonics) as a function of number of reconstructed charged particles N_{ch}^{rec} in pp and p+Pb collisions at different energies [19]. The data suggest that v_2

values are independent of the collision energy but are clearly dependent on the collision system. In particular, the v_2 in p+Pb shows a modest increase with N_{ch}^{rec} while the v_2 in pp is independent of N_{ch}^{rec}. The multiplicity dependence of v_2 is consistent with a collective response of the created particles to the initial geometry. This geometry appar
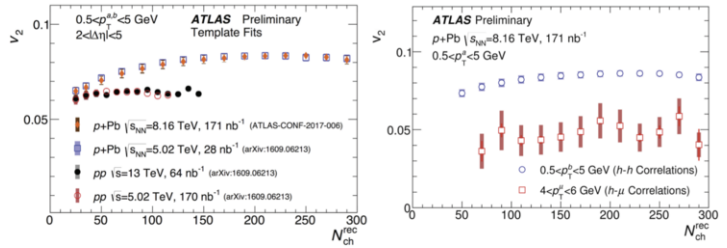

Figure 7.   Left: Charged particle $v_2\{2\}$ from pp and p+Pb collisions at various collision energies as a function of number of reconstructed charged particles. Right: $v_2\{2\}$ for heavy flavor muons compared with charged hadrons in p+Pb collisions. All results obtained using the template fit method.

ently changes with collision system but not much with collision energy.

Most ridge measurements in small systems use hadrons composed of light quarks. It is interesting to know if the ridge is also present for hadrons containing heavy quarks such as charm and bottom quarks. ATLAS has measured the two-particle ridge between heavy flavor muon in $4 < p_T < 6$ GeV and charged particles [19]. These muons, after selection cuts, are dominated by the decay of bottom hadrons. A sizable ridge and v_2 is clearly seen as shown in Fig. 7 (right), suggesting that the heavy flavor quarks also participate in the collective expansion. However the magnitude of the v_2 is much smaller than that for the light hadrons.

Another important issue concerning the ridge is whether it involves all particles in the event (collective flow) or if it arises merely from correlations among a few particles, due to non-flow. The standard multiparticle cumulant method reduces the non-flow contributions, but it is known to fail in very small collision systems or peripheral collisions in A+A system. Recently, an improved cumulant method based on the correlation between particles from different subevents separated in η has been proposed to further reduce the non-flow correlations [20]. This method was shown to be very effective in further suppressing non-flow correlations, especially those from jets and dijets.

Figure 8 shows a comparison of $c_2\{4\}$ from the standard method [21], as well as subevent methods based on two or three η-separated subevents in pp collisions at $\sqrt{s} = 5.02$ and 13 TeV, and p+Pb collisions at
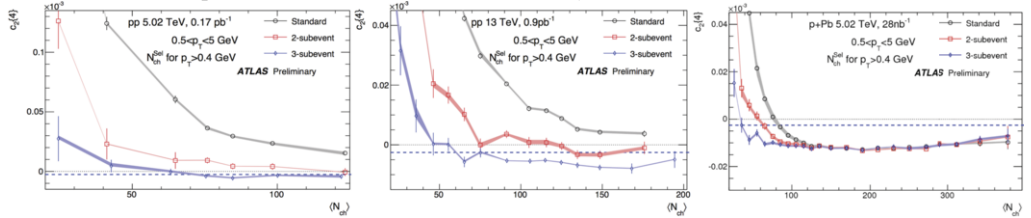

Figure 8.   The $c_2\{4\}$ compared between the three cumulant methods for 5.02 TeV pp (left panel), 13 TeV pp (middle panel) and 5.02 TeV p+Pb (left panel) data.

$\sqrt{s_{NN}} = 5.02$ TeV [22]. The results from 5.02 TeV pp collisions are similar to those from the 13 TeV pp collisions, i.e. the $c_2\{4\}$ values are smallest for the three-subevent method and are largest for the standard method. The hierarchy between the three methods is also observed in p+Pb collisions, but it is limited to the low N_{ch} region, suggesting that the influences of non-flow in p+Pb collisions are much smaller than those in pp collisions at comparable N_{ch}. In p+Pb collisions, all three methods give consistent results for $N_{ch} > 100$. Furthermore, the three-subevent methods give negative $c_2\{4\}$ values in most measured N_{ch} ranges. Comparing the three figures at the same N_{ch}, it is also clear that pp collisions at $\sqrt{s} = 5.02$ TeV has the largest non-flow, while it is smallest in p+Pb collisions at $\sqrt{s_{NN}} = 5.02$ TeV.

From the measured $c_2\{4\}$, the single particle flow harmonics is calculated as $v_2\{4\} = -\sqrt[4]{c_2\{4\}}$, which is

then combined with $v_2\{2\}$ from the 2PC measurement to infer information about the nature of

flow fluctuations in small systems. Figure 9 shows a comparison of $v_2\{4\}$ to the $v_2\{2\}$ from "template fit" and "peripheral subtraction" methods. The $v_2\{4\}$ values are smaller than the $v_2\{2\}$ from the template-fit method in both pp and p+Pb collisions. In hydrodynamic models for small collision systems, this difference can be interpreted [23] as the influence of event-by-event flow fluctuations associated with fluctuating initial conditions, which is closely related to the effective number of sources N_s for par-

Figure 9. The $v_2\{4\}$ from the three-subevent method in 13 TeV pp (left panel) and 5.02 TeV p+Pb collisions (right panel). They are compared to v_2 obtained from a two-particle correlation analysis where the non-flow effects are removed by a template fit procedure (solid circles) or with a fit after subtraction with ZYAM assumption (peripheral subtraction, solid line)

ticle production in the transverse density distribution of the initial state:

$$\frac{v_2\{4\}}{v_2\{2\}} = \left[\frac{4}{(3 + N_s)}\right]^{1/4} \tag{2}$$

Figure 10 shows the extracted N_{ch} values as a function of N_{ch} in 13 TeV pp and 5.02 TeV p+Pb collisions, using the model assumption given in Eq. 2. The extracted number of sources increases with N_{ch} in p+Pb collisions up to $N_s \sim 20$ in the highest multiplicity class. The amount of increase is about a factor of 3–4 across the entire measured N_{ch} range. Previously ATLAS has measured [24] the slope a_1 of the forward-backward multiplicity correlation in η, which is expected to scale with the number of sources for particle prduction N_f as $a_1 \propto 1/\sqrt{N_f}$. Over
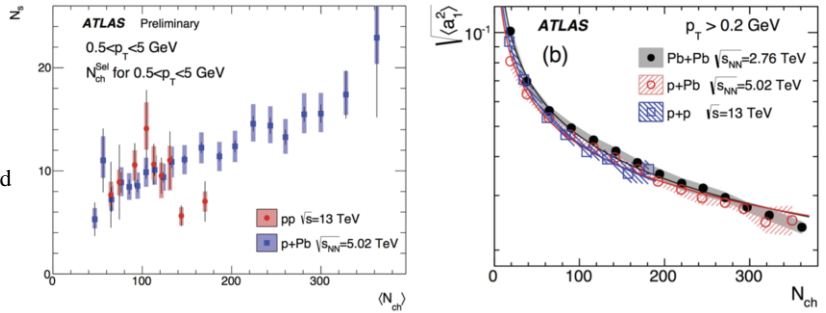

Figure 10. Left: The number of sources N_s inferred from $v_2\{2\}$ and $v_2\{4\}$ via Eq. 2 in 13 TeV pp and 5.02 TeV p+Pb collisions. Right: The slope in η of the EbyE forward-backward multiplicity fluctuation from 13 TeV pp, 5.02 TeV p+Pb and 2.76 TeV Pb+Pb collisions.

the same multiplicity range, a_1 value decreases by a factor of ~ 2, corresponding to an increase of N_f by a factor of four. Therefore it is an intriguing question whether these two sources are related: N_s the number of sources responsible for the eccentricity driving the transverse collective flow, and the N_f, the number of sources responsible for particle production as a function of η.

Finally if the ridge is related to the collective expansion of the systems, it would be interesting to perform Hanbury Brown and Twiss (HBT) correlations to measure the size of particle emission sources. ATLAS presented a detailed study of the three-dimensional HBT measurement in high-multiplicity p+Pb collisions [25]. Several important observations have been made, including a first observation of a small but significant out-long cross-correlation R_{ol} which reflects the Forward-Backward (FB) asymmetry of the sources in p+Pb collisions (see Fig. 11(left)). The measurement was also extended to azimuthal dependent HBT with respect to the 2nd-order event plane Ψ_2 determined in the Pb-going direction. Many observables

have been studied, including the $R_{\mathrm{out}}(\phi-\Psi_2)$ shown in Fig. 11(right). The R_{out} is found to be significantly smaller along the in-plane direction than along the out-of-plane direction, suggesting that the sources expand more explosively along the event-plane direction. This

Figure 11. Left: The cross term, R_{ol}, as a function of the pair rapidity in several centrality intervals in p+Pb collisions. Right: The outwards HBT radius R_{out} as a function of angular w.r.t the second-order event plane determined in the Pb-going direction in p+Pb collisions.

behavior is qualitatively similar to observations made in the A+A collisions, and is consistent with the hydrodynamical picture.

7. Conclusion
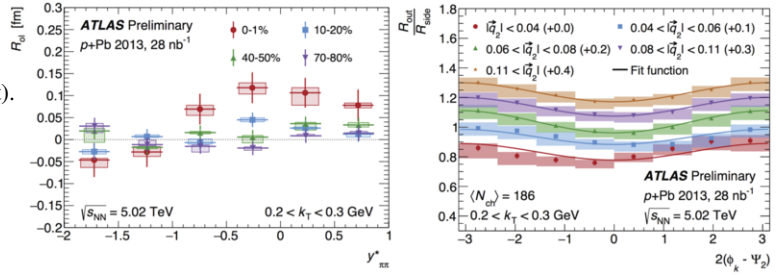
ATLAS produced many new results covering pp, p+Pb and Pb+Pb collisions at various collision energies. These results provide new information on the initial state of p+Pb and Pb+Pb collisions, the jet quenching and quarkonium production, longitudinal collective flow dynamics in PbPb collisions, as well as comprehensive studies and an improved understanding of the collectivity in small collision systems.

This research is supported by NSF under grant numbers PHY-1305037 and PHY-1613294.

References

[1] ATLAS Collaboration, arXiv: 1702.01625 [hep-ex]; M. Dyndal, these proceedings.
[2] ATLAS Collaboration, A. Angerami, these proceedings; ATLAS-CONF-2017-011.
[3] ATLAS Collaboration, Z. Citron, these proceedings; ATLAS-CONF-2017-010.
[4] ATLAS Collaboration, M. Spousta, these proceedings; ATLAS-CONF-2017-009; ATLAS-CONF-2017-012.
[5] ATLAS Collaboration, R. Slovak, these proceedings; ATLAS-CONF-2017-004; ATLAS-CONF-2017-005.
[6] ATLAS Collaboration, arXiv:1702.00674 [hep-ex].
[7] ATLAS Collaboration, P. Steinberg, these proceedings; ATLAS-CONF-2016-110.
[8] ATLAS Collaboration, J. Lopez, these proceedings; ATLAS-CONF-2016-109.
[9] ATLAS Collaboration, ATLAS-CONF-2015-050.
[10] P. Bozek, W. Broniowski, and J. Moreira, Phys. Rev. **C83** (2011) 034911, arXiv:1011.3354 [nucl-th].
[11] J. Jia and P. Huo, Phys. Rev. C **90** (2014) 034915, arXiv:1403.6077 [nucl-th].
[12] J. Jia, P. Huo, G. Ma, and M. Nie, arXiv:1701.02183 [nucl-th].
[13] CMS Collaboration, Phys. Rev. C **92** (2015) 034911, arXiv:1503.01692 [nucl-ex].
[14] ATLAS Collaboration, P. Huo, these proceedings; ATLAS-CONF-2017-003.
[15] ATLAS Collaboration, S. Mohapatra, these proceedings; ATLAS-CONF-2017-003.
[16] ATLAS Collaboration, Phys. Rev. C **90** (2014) 044906, arXiv:1409.1792 [hep-ex].
[17] ATLAS Collaboration, arXiv:1609.06213 [nucl-ex].
[18] PHENIX Collaboration, A. Adare et al., Phys. Rev. C **78** (2008) 014901, arXiv:0801.4545 [nucl-ex].
[19] ATLAS Collaboration, B. Cole, these proceedings; ATLAS-CONF-2017-006.
[20] J. Jia, M. Zhou, and A. Trzupek, arXiv:1701.03830 [nucl-th].
[21] ATLAS Collaboration, A. Trzupek, these proceedings; ATLAS-CONF-2017-007.
[22] ATLAS Collaboration, M. Zhou, these proceedings; ATLAS-CONF-2017-002.
[23] L. Yan and J.-Y. Ollitrault, Phys. Rev. Lett. **112** (2014) 082301, arXiv:1312.6555 [nucl-th].
[24] ATLAS Collaboration, arXiv:1606.08170 [hep-ex].
[25] ATLAS Collaboration, M. Clark, these proceedings; ATLAS-CONF-2016-027; ATLAS-CONF-2017-008.